Briefing Space Weather - 2022/05/02

Sun

Responsible: José Cecatto

04/25 – 2 M-flares (AR 2995/2993); Fast (=< 500 km/s) wind stream; 7 CME c.h.c. toward the Earth – 1 partial halo;
04/26 – Fast (=< 450 km/s) wind stream; 5 CME c.h.c. toward the Earth;
04/27 – Fast (=< 500 km/s) wind stream; 12 CME c.h.c. toward the Earth – 2 partial halo;
04/28 – Fast (=< 550 km/s) wind stream; 4 CME c.h.c. toward the Earth – 1 partial halo;
04/29 – 2 M-flares (AR 2996); Fast (=< 550 km/s) wind stream; 5 CME c.h.c. toward the Earth – 1 partial halo;
04/30 – 4 M-flares and 1 X1-flare (AR 2994); Fast (=< 550 km/s) wind stream; 11 CME c.h.c. toward the Earth;
05/01 – Fast (=< 500 km/s) wind stream; 12 CME c.h.c. toward the Earth;
05/02 – Fast (=< 500 km/s) wind stream; 5 CME c.h.c. toward the Earth;
Prev.: Fast wind expected up to May 04-05; for while good (15% M, 1% X) probability of M / X flares next 2 days; also, occasionally other CME can present component toward the Earth.
c.h.c. – can have a component

Responsible: Douglas Silva

WSA-ENLIL (CME 2022-04-26T14:53)
● The simulation results indicate that the flank of CME will reach the DSCOVR mission between
2022-04-30T01:30Z e 2022-04-30T15:30Z.
WSA-ENLIL (CME 022-04-27T08:48Z, 2022-04-27T14:53Z)
● The simulation indicates that the combined Coronal Mass Ejections will reach the DSCOVR
mission between 2022-04-30T01:30Z and 2022-04-30T15:30Z.
WSA-ENLIL (CME 2022-04-29T07:38Z)
● The simulation results indicate that the flank of CME will reach the DSCOVR

mission between
2022-04-30T21:15Z and 2022-05-01T12:47Z.

Coronal holes (SPOCA):

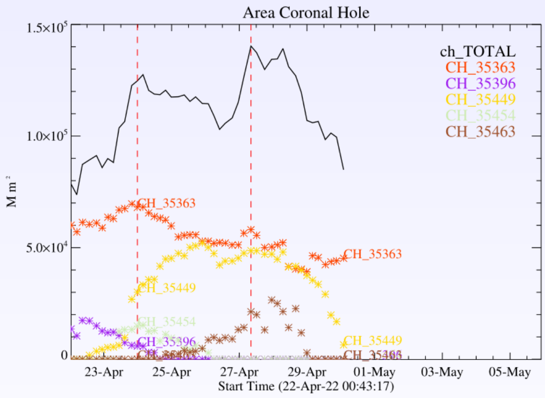

Figura: The solid line in black shows the products of the sum of areas for each detection interval performed by SPOCA between April 22 and May 2, 2022.

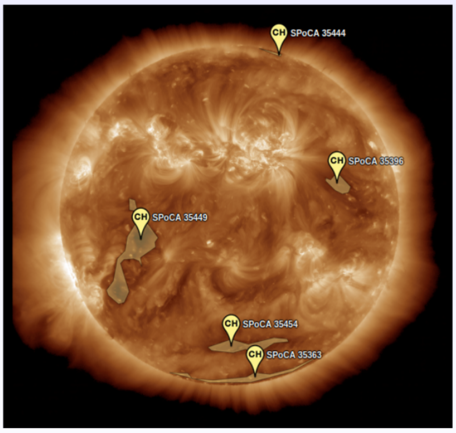

Figura: Above the 193 Å image of the Sun are highlighted coronal holes observed by SPOCA around 00:00 UT on April 24, 2022.

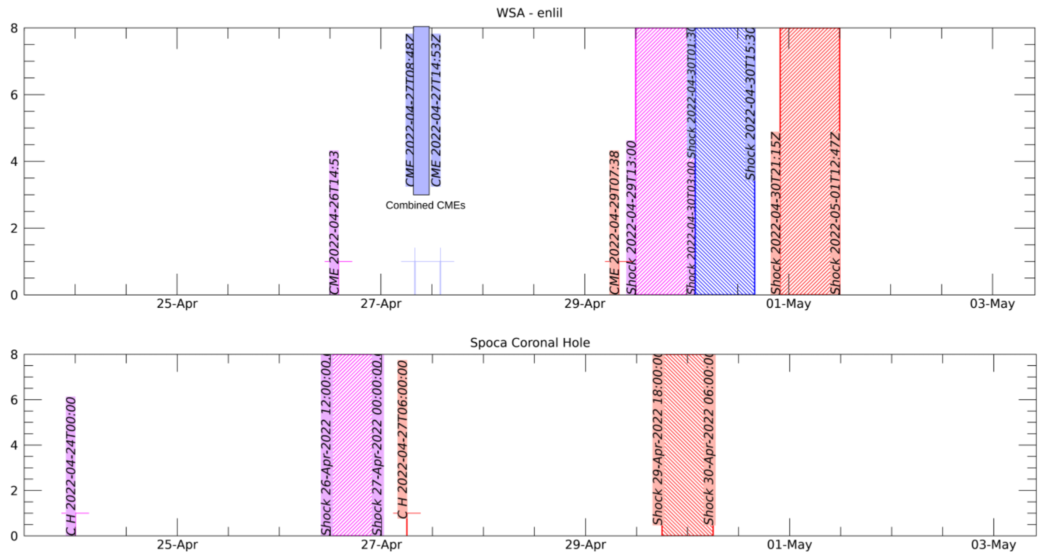

Radiation Belts

Responsible: Ligia Alves Da Silva

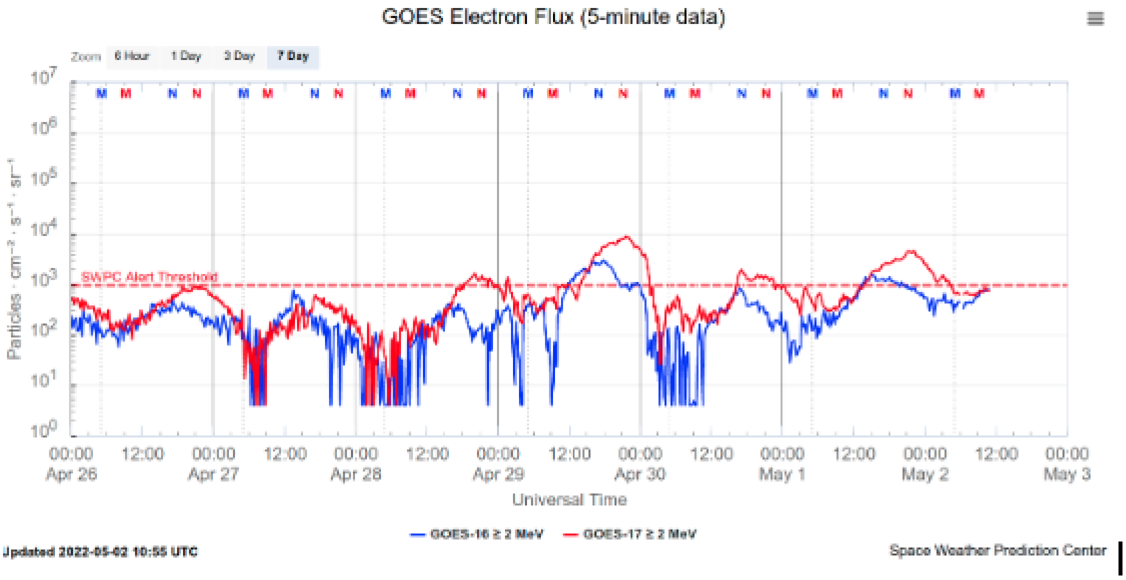

Figure 1: High-energy electron flux (> 2MeV) obtained from GOES-16 and GOES-17 satellite.
Source: https://www.swpc.noaa.gov/products/goes-electron-flux

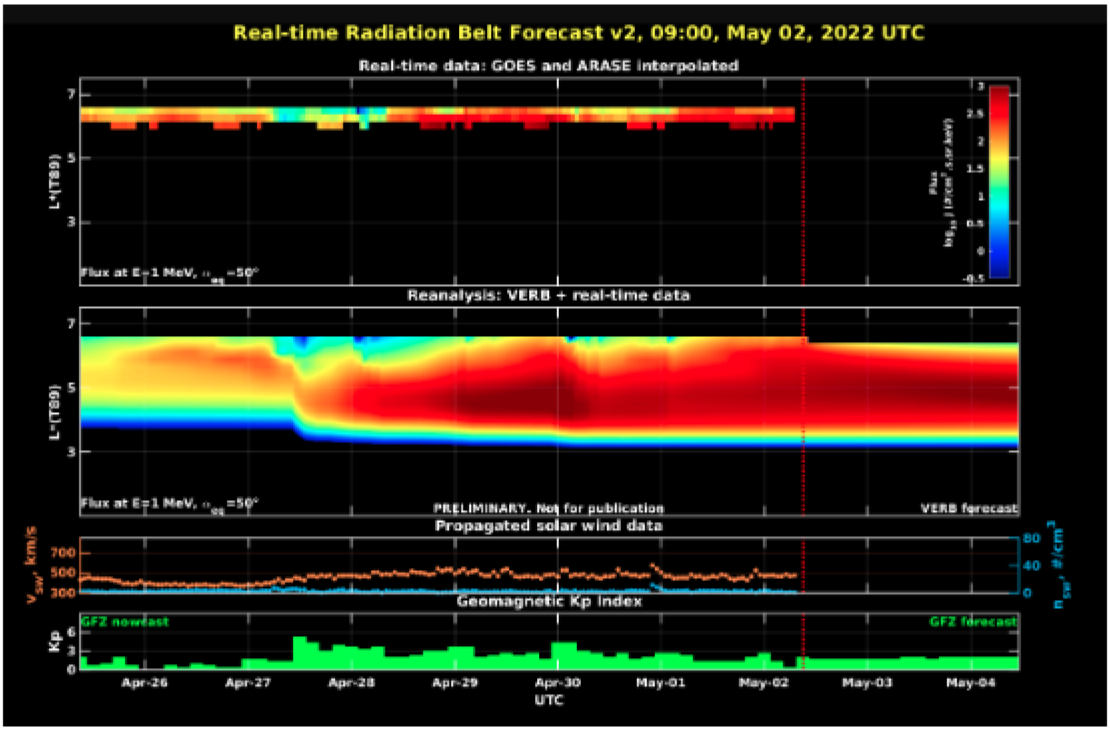

Figure 2: high-energy electron flux data (real-time and interpolated) obtained from ARASE, GOES-16, GOES-17 satellites. Reanalysis's data from VERB code and interpolated electron flux. Solar wind velocity and proton density data from ACE satellite.
Source: https://rbm.epss.ucla.edu/realtime-forecast/

High-energy electron flux (>2 MeV) in the outer boundary of the outer radiation belt obtained from geostationary satellite data GOES-16 and GOES-17 (Figure 1) is stable between the thresholds 102 and 103 particles/(cm2 s sr) until the beginning of April 27th. Two electron flux decreases were observed on April 27th and 28th. After the second electron flux decrease, an increase is observed that persists around 103 particles/(cm2 s sr) until today, presenting only one peak that reached 104 particles/(cm2 s sr) at the end of April 29th, followed by a dropout on April 30th.

The GOES-16, GOES-17, and Arase satellite data are analyzed and interpolated to observe the high-energy electron flux variability (1 MeV) in the outer radiation belt (Figure 2). Additionally, the VERB code rebuilds this electron considering the Ultra Low Frequency (ULF) waves' radial diffusion. The simulation (VERB code) shows that the first electron flux decrease observed from April 27th reached L-shell = 5.0, the second (April 28th) reached L-shell = 6.0, and the third (April 30th) L-shell = 6.5. These electron flux variability occurred concomitantly with the arrival of solar wind structures (coronal mass ejections and high-speed streams) and ULF wave activities. However, it is important to point out that the data from the ARASE satellite are not available for the week under analysis to confirm the L-shell level of these electron flux variabilities.

ULF waves in the Magnetosphere

Responsible: José Paulo Marchezi

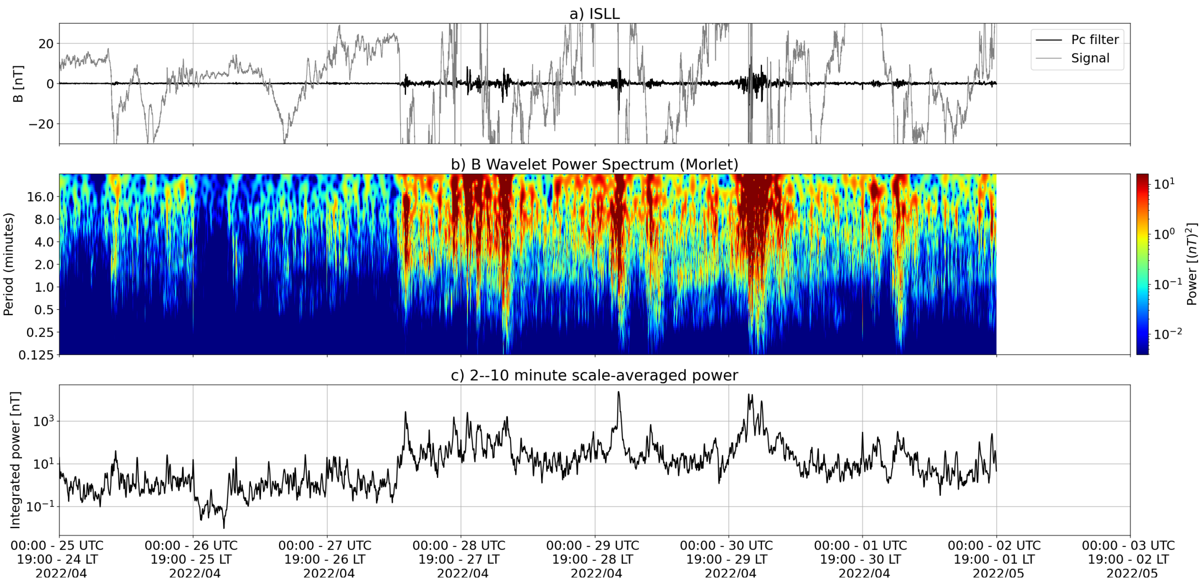

a) signal of the total magnetic field measured in the ISLL Station of the CARISMA network in gray, together with the fluctuation in the range of Pc5 in black. b) Wavelet power spectrum of the filtered signal. c) Average spectral power in the ranges from 2 to 10 minutes (ULF waves).

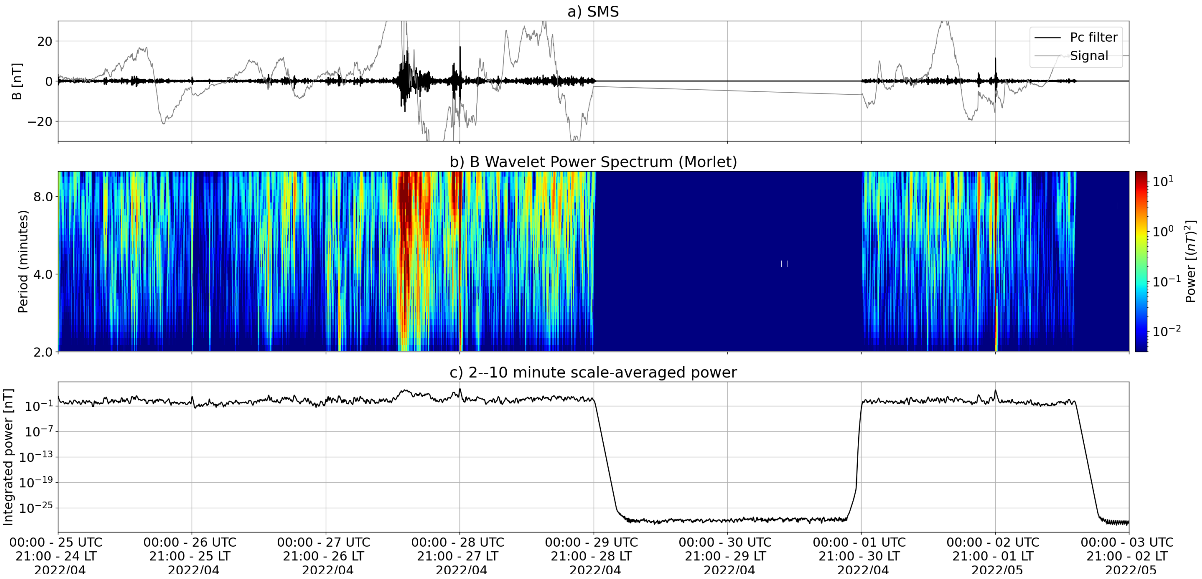

a) signal of the total magnetic field measured in the SMS Station of the EMBRACE network in gray, together with the fluctuation in the range of Pc5 in black. b) Wavelet power spectrum of the filtered signal. c) Average spectral power in the ranges from 2 to 10 minutes (ULF waves).

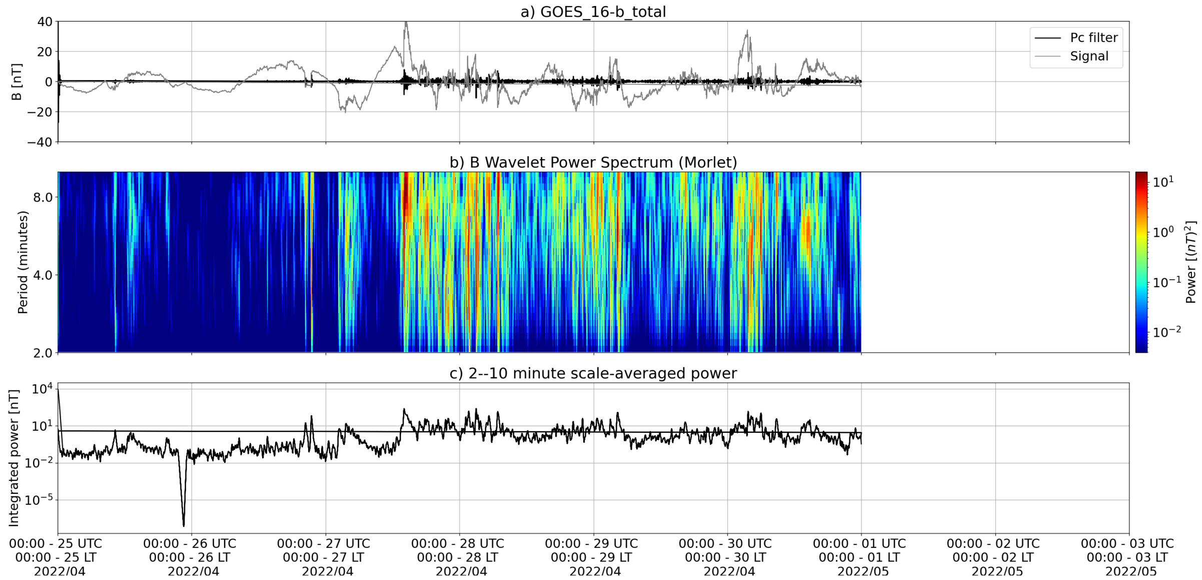

a) signal of the total magnetic field measured by the GOES 16 satellite, together with the fluctuation in the range of Pc5 in black. b) Wavelet power spectrum of the filtered signal. c) Average spectral power in the ranges from 2 to 10 minutes (ULF waves).

The ULF wave activity shows an increase in power from the 27th of April in the form of irregular and short-lived pulsations, detected from high latitudes to the magnetometers at low latitudes of the EMBRACE network (Figure 2, SMS). The activity continues until the 29th of April, new increases in ULF power are observed at high latitudes and with an impulsive characteristic on the 28th, with fluctuations remaining until the 29th of April. On the 30th, there is a new increase in spectral power, now with continuous characteristics, mainly at high latitudes and also detected by the GOES satellite. This period is under the effect of a corrosive interaction region (CIR) and also periods with increasing density of the solar wind and component of the magnetic field of the solar wind predominantly in the south direction.

EMIC waves in the Magnetosphere

Responsible: Claudia Medeiros

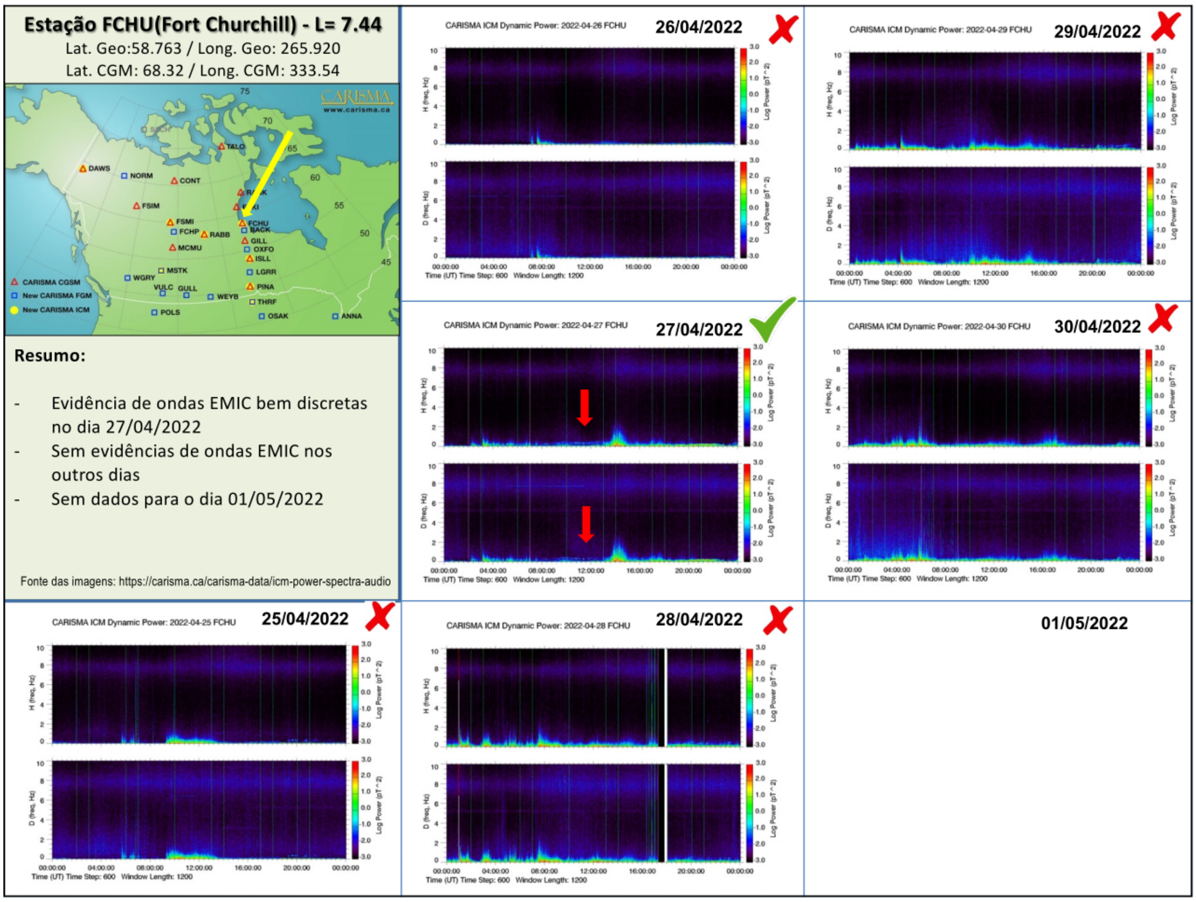

Geomagnetism

Responsible: Livia Ribeiro Alves

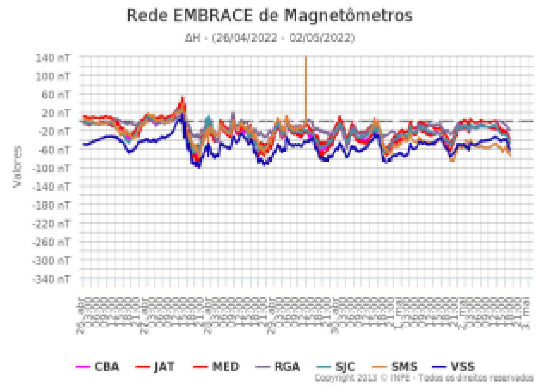
Rede EMBRACE de Magnetômetros
ΔH - (26/04/2022 - 02/05/2022)
Valores
CBA
JAT
MED
RGA
SJC
SMS
VSS
Copyright 2013 © INPE - Todos os direitos reservados

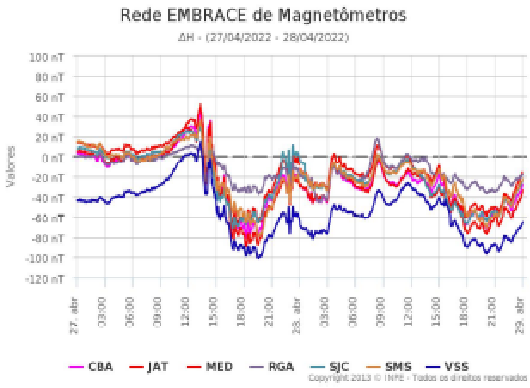
Rede EMBRACE de Magnetômetros
ΔH - (27/04/2022 - 28/04/2022)
Valores
CBA
JAT
MED
RGA
SJC
SMS
VSS
Copyright 2013 © INPE - Todos os direitos reservados

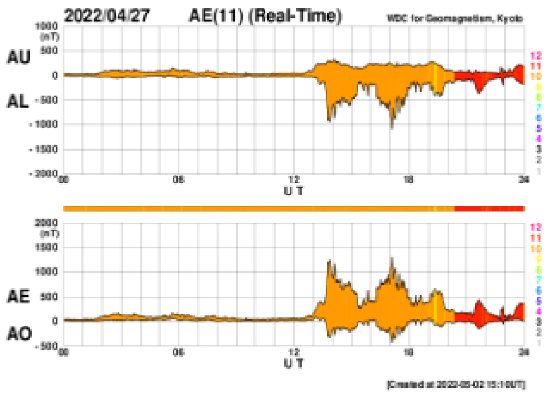
2022/04/27
AE(11) (Real-Time)
WDC for Geomagnetism, Kyoto
AU
AL
AE
AO
U T
[Created at 2022-05-02 15:10UT]

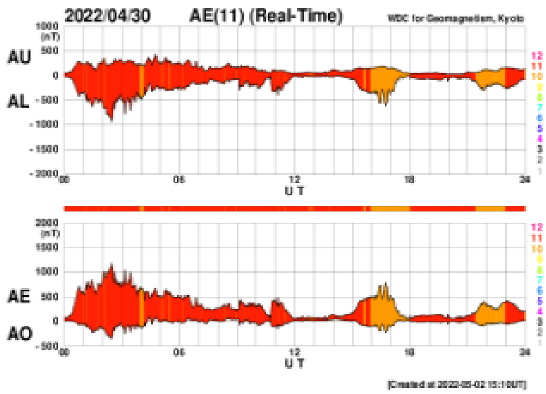
2022/04/30
AE(11) (Real-Time)
WDC for Geomagnetism, Kyoto
AU
AL
AE
AO
U T
[Created at 2022-05-02 15:10UT]

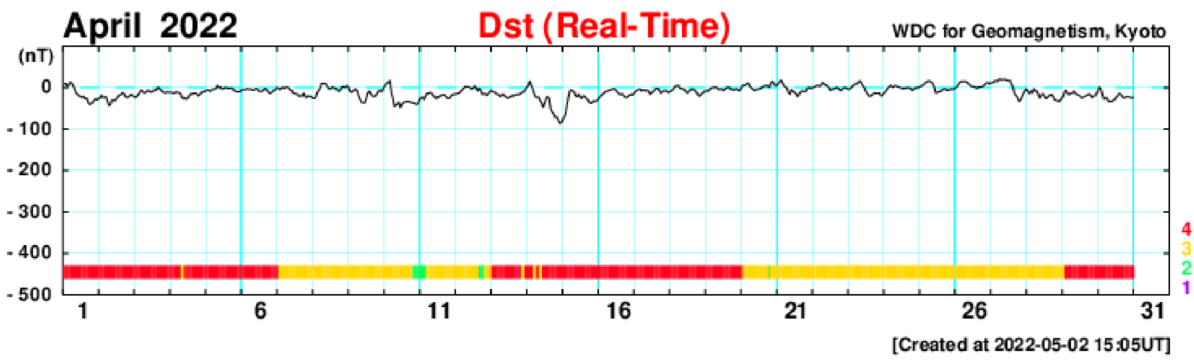
April 2022
Dst (Real-Time)
WDC for Geomagnetism, Kyoto
(nT)
[Created at 2022-05-02 15:05UT]

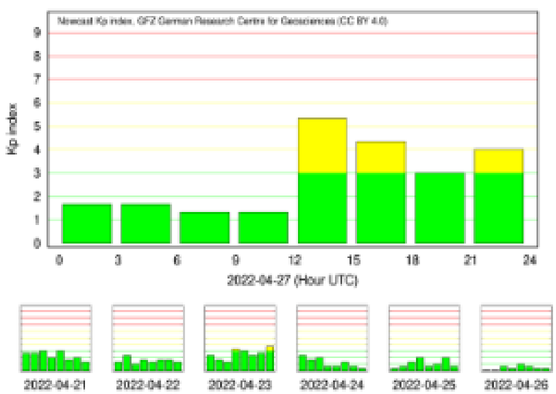
Nowcast Kp index, GFZ German Research Centre for Geosciences (CC BY 4.0)
Kp index
2022-04-27 (Hour UTC)
2022-04-21
2022-04-22
2022-04-23
2022-04-24
2022-04-25
2022-04-26

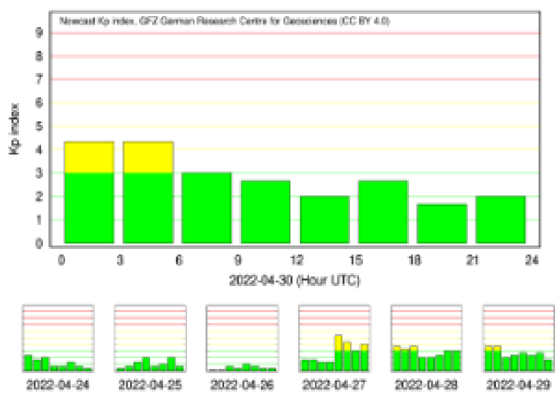
Nowcast Kp index, GFZ German Research Centre for Geosciences (CC BY 4.0)
Kp index
2022-04-30 (Hour UTC)
2022-04-24
2022-04-25
2022-04-26
2022-04-27
2022-04-28
2022-04-29

- Data from the Embrace magnetometer network showed instabilities throughout the period, with some events highlighted:
  27th, drop in H component in all seasons, up to -100 nT
- Geomagnetic activity was more disturbed on 05/27, with the Dst index reaching its minimum value of -30 nT in . Highest Kp of the week was 5+ recorded on 04/27
- The auroral activity was intensified in the period from 04/27 to 04/30, highlighting these two days.
- Magnetic field measured in the orbit of the GOES satellite showed disturbances on 04/27.

Scintillation S4

Responsible: Siomel Savio Odriozola

In this report on the S4 scintillation index, data from SLMA in São Luiz/MA, STNT in Natal/RN, STSN in Sinop/MT and SJCE in São José dos Campos/SP are presented. The S4 index tracks the presence of irregularities in the ionosphere having a spatial scale ~ 360 m.

The stations STSN, STNT and SJCE did not present relevant values of the S4 index throughout the week. In the SLMA station, there were two cases with S4 values above 0.4. The most important was recorded in the morning of 04/25 (Figure 1, upper panel). In the lower panel of Figure 1, the affected satellites located to the north and south of the SLMA station appear. Ionograms and TEC
maps at the same time and place did not show any evidence that explains the behavior of S4 in SLMA during the morning of 04/25.

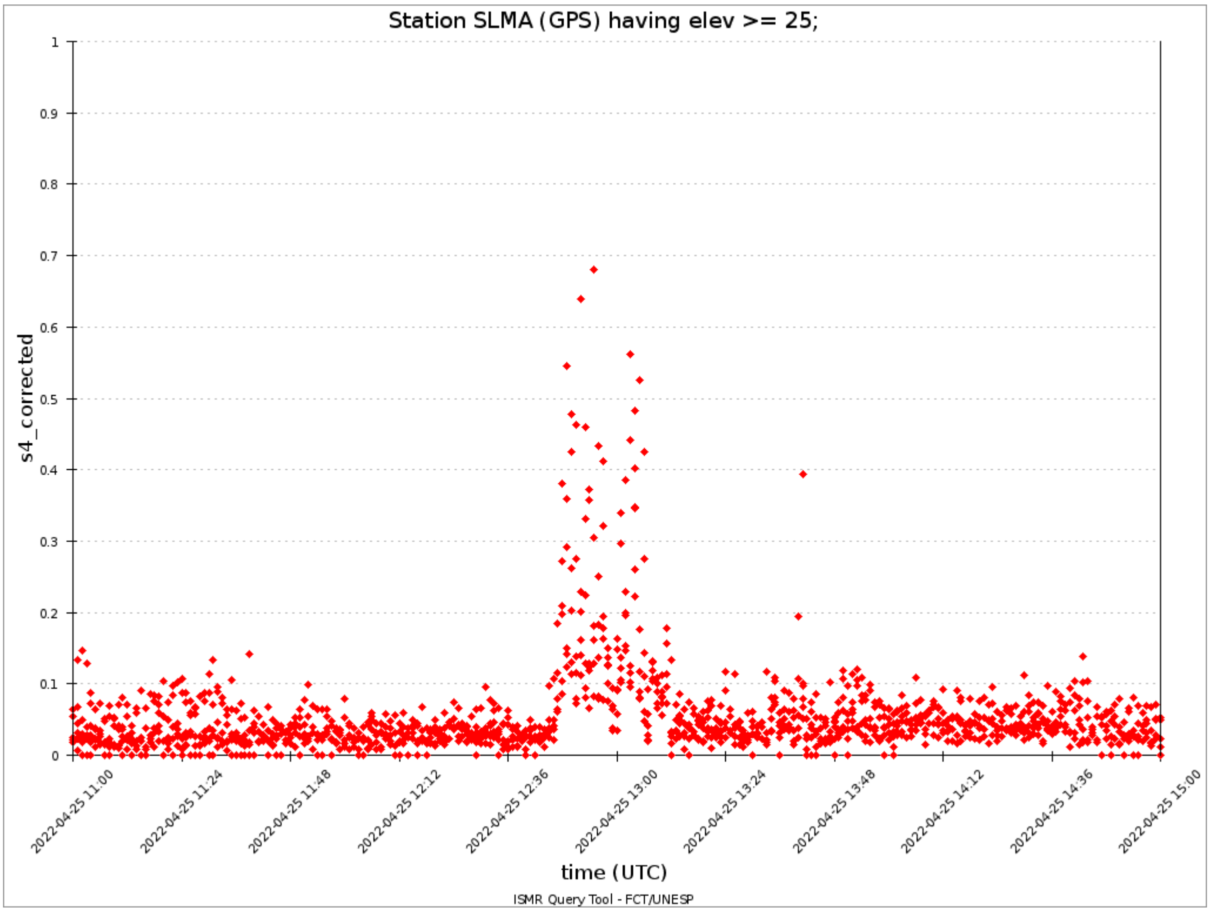
Station SLMA (GPS) having elev >= 25;
s4_corrected
time (UTC)
ISMR Query Tool - FCT/UNESP

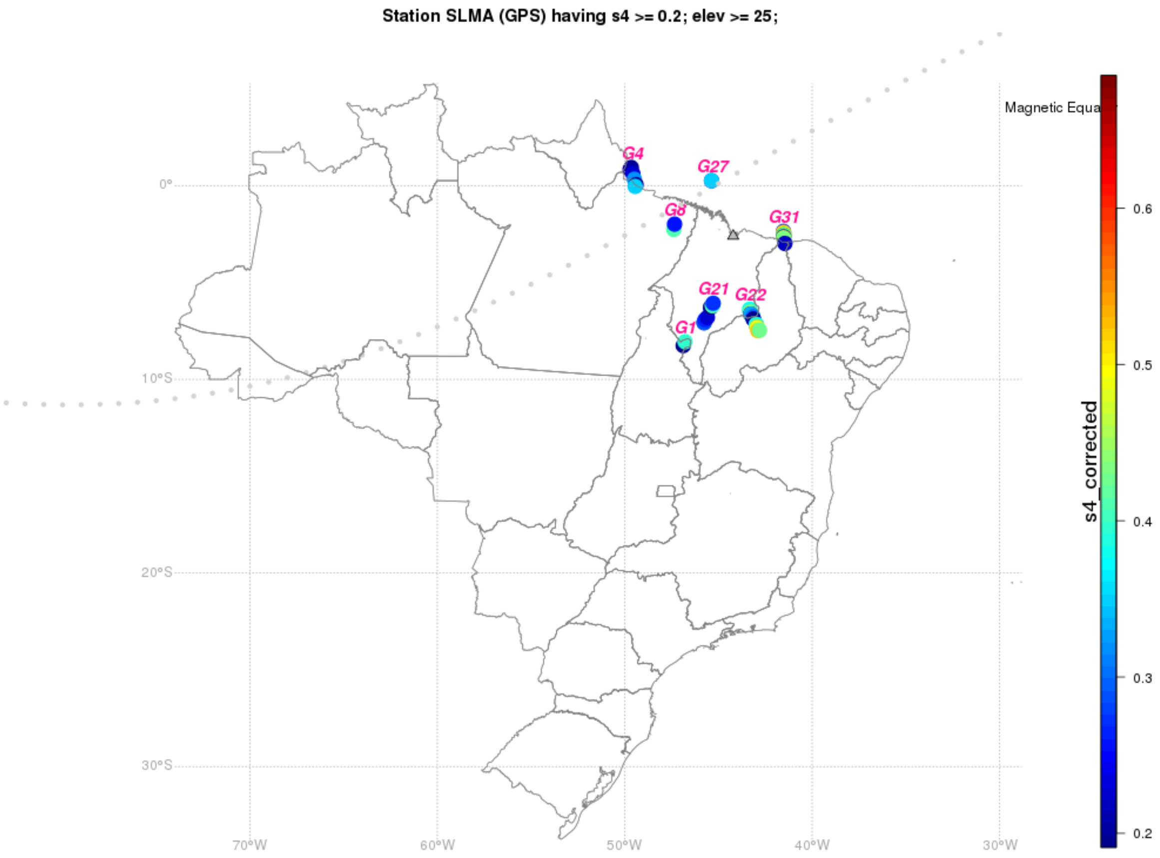

Figure 1: S4 index values corresponding to the GPS constellation for the SLMA station on 04/25. Between 1100 and 1500 UT (top panel). In the lower panel the map of S4 values > 0.2 for GPS satellites with elevation > 25o in the receiver's field of view from the same station of the upper panel and for the same time interval.

All-Sky Imager

Responsible: LUME

All-Sky Imager EPBs Observation || Apr 24 - Apr 30, 2022
Observações das EPBs por meio do imageador All-Sky -
|| 24 apr - 30 abril, 2022

Observatory Observatório	Apr 24 Abril 24	Apr 25 Abril 25	Apr 26 Abril 26	Apr 27 Abril 27	Apr 28 Abril 28	Apr 29 abril 29	Apr 30 abril 30
CA	✗	✗	✗	✗	✗	✗	✗
BJL	✓❍	✓❍	✗	✗	✗	✗	✗
CP	✓●	✓❍	✓◗	✓❍	✓◗	✓●	✓●
SMS	✗	✗	✗	✗	✗	✗	✗

CA	São João do Cariri
BJL	Bom Jesus da Lapa
CP	Cachoeira Paulista
SMS	São Martinho da Serra
✓	Observation - Observação
✗	No Observation - Sem Observação
❍	Clear sky - Céu limpo
◗	Partly Cloudy - Parcialmente Nublado
●	Cloudy - Nublado
✺	Blur image - Desfocar Imagem

- At the São João do Cariri observatory, there were no observation during the entire week.
- At the Bom de Jesus da Lapa observatory between 26th of April and the 30th of April, there there no observation. There were no observe plasma bubbles structures observed on the days that there were observations.
- At the Cachoeira Paulista no plasma bubbles were observed during the entire week even though there were observation. Day 24, 29 and 30 were cloudy.
- Finally, at the observatory of São Martinho da Serra, no plasma bubble structures were observed during the entire week.

TEC

- Plasma bubbles were observed throughout the period for the days with TEC map covering the entire Brasil. However, as the bubble seasonality is at the end, thus the plasma bubbles have small spatial dimensions and are difficult to observe on TEC maps.

ROTI

Responsible: Carolina de Sousa do Carmo

The ROTI (Rate of TEC index) is an index based on the variation of the TEC (Total Electron Content) (Pi et al., 1997). This index is used to detect ionospheric irregularities, such as
plasma bubbles. The ROTI index shows a good correlation with the S4 scintillation index (e.g., Carrano et al., 2019). **Table 1** shows the week's summary (April 24-30, 2022) according to the ROTI index, showing the times of detection of ionospheric irregularities in the South American sector. In addition, Figures 1 shows the keograms of the ROTI index, for fixed geographic latitudes 5°S and 15°S, with geographic longitude versus universal time (UT).

Week	Day	Time of occurrence (UT)
Sunday	2022/04/24	-
Monday	2022/04/25	01:40-04:20
Tuesday	2022/04/26	01:40-05:30
Wednesday	2022/04/27	-
Thursday	2022/04/28	-
Friday	2022/04/29	No data
Saturday	2022/04/30	No data

Table 1 – Weekly Summary (April 24-30, 2022).

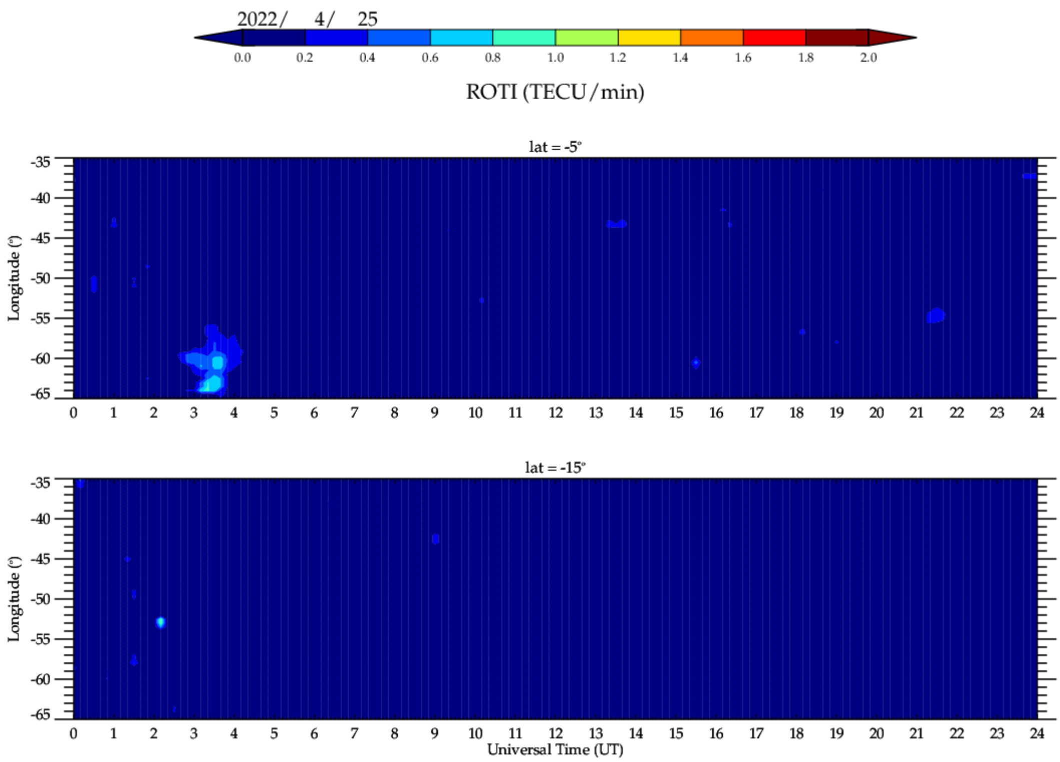

Figure 1 - Keogram of the ROTI index for fixed geographic latitudes 5°S and 15°S, on April 25, 2022.

In summary, the 25th and 26th of April had structures similar to plasma bubbles, at times indicated in Table 1, in the northern region of Brazil. However, this region has low coverage of GNSS receivers, facilitating the propagation of errors and the border effect in the maps.